

STOCHASTIC AND TUBE MPCs FOR TURBINE CONTROL

Project Information	
Acronym - Title	ICONIC – Smart, Aware, Integrated Wind Farm Control Interacting with Digital Twins
Project no.	101122329
Call // Topic	HORIZON-CL5-2022-D3-03 // HORIZON-CL5-2022-D3-03-04
Type of action // Service	HORIZON-RIA // CINEA/C/02
Project duration // starting and end date	48 months // 1/12/2023 – 30/11/2027
Website	www.iconicwind.org
Deliverable Information	
Number & Title	D12 / D3.2 - Stochastic and tube MPCs for turbine control
WP number and title	WP3 – Advanced wind turbine control with load-reduction abilities
Author	Torben Knudsen
Description	Stochastic and Tube MPCs for turbine control. It corresponds to T3.2: Stochastic and tube MPCs for turbine control with load reduction.
Lead Beneficiary	AAU
Type	R: Document, report
Dissemination Level	PU: Public
Status	Final
History of Changes	
Version 0.1	Draft created by AAU (25.04.2025)
Version 0.2	Approval by SB after corrections (23.05.2025)
Version 1	Approved by General Assembly (30.05.2025)

Copyright

This work is licensed under the [Creative Commons Attribution 4.0 International License](https://creativecommons.org/licenses/by/4.0/).



**Funded by
the European Union**

Views and opinions expressed are however those of the author(s) only and do not necessarily reflect those of the European Union or the granting authority. Neither the European Union nor the granting authority can be held responsible for them.

TABLE OF CONTENT

1	Preface	3
2	Article: “Stochastic and tube MPCs for turbine control”	4
3	Article: Stochastic MPC with focus on probabilistic constraints"with application to.....	27
	wind turbine control	

1 PREFACE

Deliverable D3.2 is organized in three parts.

1. The first part is this document including the front matter with the mandatory project and deliverable information.
2. The second part is dedicated to necessary development of the SMPC method. This part is documented in a paper for the conference ACC25. This part is a pdf file produced by LaTeX.
3. The third part includes the full contents of the deliverable. It begins with a summary of the theory and method ACC25 paper. The main part analyzes the differences between the developed SMPC controller with only constraints and two other controllers. One SMPC without probabilistic constraints but with penalty on rotational speed and then the OpenFAST ROSCO controller which is used for bench-marking. This part is also a pdf file produced by LaTeX.

D3.2 Stochastic and tube MPCs for turbine control

Torben Knudsen
Automation and Control
Department of Electronic Systems
Aalborg University

May 23, 2025



AALBORG UNIVERSITY
DENMARK

Abstract

A stochastic model predictive control (SMPC) is developed where limits/constraints are specified with a probability for the real, not predicted as in traditional MPC, states exceeding the limits. This will be particularly useful in full load where it is proposed not to follow a set point for the rotational speed but only use the probabilistic limits as an allowed zone for the speed. Blade pitching will then not be done continuously to follow the speed set point but only when the probability of leaving the zone is too large. This will potentially save blade and tower fatigue from pitching and increasing energy around the rated wind speed.

Contents

1	Preface	2
2	Introduction	3
3	Development of SMPC methods and algorithms	3
4	Results for the benchmark model OpenFAST/ROSCO	3
5	Comparing SMPC and "standard" control performance using the OpenFAST 5MW virtual wind turbine	4
5.1	Simulation software	8

5.2	Objectives	9
5.3	Operational conditions	9
5.4	Controller configuration	10
5.5	Results for the model in the paper with only speed and wind states and speed constraints	10
5.5.1	Tuning of the KF	11
5.5.2	Assessment of the KF	11
5.5.3	Assessment of the controller performance	12
5.6	Results for the model in the paper with only speed and wind states and speed penalty . .	17
5.6.1	Assessment of the KF	17
5.6.2	Assessment of the controller performance	19
6	Conclusion	20
7	Future work	21
A	Comparing SMPC-OP to SMPC-OC	22

Abbreviations

CV	Coefficient of Variation	PI	Proportional Integral
DEL	Damage Equivalent Load	PL	Partial Load
DOF	Degree Of Freedom	RMSE	Root Mean Square Error
DOF	Degrees Of Freedom	SMPC	Stochastic Model Predictive Control
EKF	Extended Kalman Filter	SMPC-OC	SMPC with only constraint
EWS	Effective Wind Speed	SMPC-OP	SMPC with only penalty
FL	Full Load	SS	State Space
KF	Kalman Filter	Std	Standard Deviation
MAD	Median Absolute Deviation	WT	Wind Turbine
MPC	Model Predictive Control		

1 Preface

Deliverable D3.2 is organized in three parts. First the front matter including the mandatory project information, then this report with result of applying the theory and methods documented in a ACC25 paper which is the last part. The pdf version of the deliverable includes all parts in the above order.

2 Introduction

The research in this deliverable can be separated in two tasks. One task is dedicated to necessary development of the SMPC method. The next task analyzes the differences between the developed SMPC

controller with only constraints and two other controllers. One SMPC without probabilistic constraints but with penalty on rotational speed and then the OpenFAST ROSCO controller which is used for benchmarking.

3 Development of SMPC methods and algorithms

This part is documented in details in the paper Knudsen et al. [2025] to be presented at the conference ACC25 (American Control Conference) in a invited wind energy session. The paper can be found in the share point via (SMPC method paper). Below follows a summary of the ACC25 paper.

The paper contributes to three challenges using probabilistic constraints in SMPC and illustrates the points made with an example from wind turbine (WT) control.

The current research on SMPC identifies the growth of the prediction covariance as a major problem as it is claimed to generally lead to infeasibility for relevant predicting horizons. The paper explains that the *conditional probability* of respecting the constraints can be smaller than 0.5 even if the *unconditional probability* is close to 1. In this case the constraints are loosened not tightened when the prediction variance increase and there is no feasibility problem at all. In case the conditional probability of respecting the constraints are larger than 0.5 so the constraints are tightened the solution is to truncated the covariance update after a suitable number of samples as the controller after some samples anyway has a better prediction.

The *unconditional probability* of respecting constraints are relevant in applications but the design parameter is the probability *conditioned on present measurements*. This is generally a overseen problem. The paper develops an approximate relation between the two probabilities which makes it easy to find a good initial value for the conditional probability to test and tune in practice or simulation as demonstrated in the application example.

An important point made in the paper is that a given *unconditional probability* for respecting constraints can be obtained by many controller designs. For conventional set point following controllers the distribution of all signals will be close to Gaussian if the disturbance are and the system is close to linear. The SMPC controller that mainly, or only, use constraints to limit the variation of the controlled variable will have clearly non Gaussian distributions for both inputs and controlled variables. This is demonstrated in the WT application example. The difference between constraint based SMPC and conventional controllers are in the distributions and in the ease of design. the paper have given contributions to the latter as demonstrated in the simple WT example.

However, if the change in distributions can be exploited for improving fatigue and WT performance in general calls for a more sophisticated model which is a subject for future research.

4 Results for the benchmark model OpenFAST/ROSCO

The NREL ROSCO controller Abbas et al. [2022] is used as a benchmark because it is recognized as the state of art. ROSCO runs in a fairly basic mode with TSR Tracking (`VS_ControlMode 3`) in partial load (PL) based on a extended Kalman filter (EKF) (`WE_Mode 2`) of the wind speed. In FL it runs with constant generator torque (`VS_ConstPower 0`) and proportional integral (PI) collective pitch control (`PC_ControlMode 1`). A pitch rate limit at 10 deg/sec. is used. The parenthesis refers to the associated parameters in the DISCON.IN setup file. The mean wind speed used is 17 m/s and the turbulence is class B.

With this setup a simulation using OpenFAST (without Simulink) has been run for 600 sec. The reason not to use the MATLAB/Simulink version of OpenFAST is that the ROSCO controller is not maintained and supported. Consequently, it is not safe to use as a benchmark. Figure 1 shows the time plot for the selected signals explained in table 1.

The main statistics for these signals are seen in table 2. The numbers marked with DEL is the scaled damage equivalent load (DEL) included in the table. This measure is based on rain flow counting using MATLAB RAINFLOW and the below formula where n_i is the count of range f_i and m is the Wöhler coefficients which here is 10 for blades (glass fiber) and 4 for the tower (steel).

$$\text{DEL} = \left(\sum_i n_i f_i^m \right)^{\frac{1}{m}} . \quad (1)$$

Notice that the number in row DEL for blade pitch is the total traveled angle which is a proxy for wear on the pitch system.

Notice that the wind speed Wind1VelX is the point wind speed centered at hub height in the undisturbed wind field generated by TurbSim. This wind speed can not be measured in reality. The next wind speed RtVAvgxh is the averaged over the rotor and relative to the rotor which will be moving. Neither this wind speed can be measured in reality but it is close to the *effective wind speed* which is useful to estimate from other measurable signals.

The rotor effective wind speed (EWS) is defined as the average wind speed which would have been across the rotor plane if the rotor and turbine was not there. An alternative interpretation is the constant ambient wind speed which would give the rotor thrust and torque as it experience. The estimate of EWS is important for the controller. In ROSCO it is estimated using only generator speed, torque and blade pitch as input to a EKF. The EWS estimate from ROSCO is show in figure 2 where it is compared to the signal RtVAvgxh which is the OpenFAST signal which is closets to EWS. The statistics for this comparison is also shown in table 3. For completeness it is also compared to the hub point wind speed Wind1VelX which is of cause far less relevant. The MAD scaled row is the median absolute deviation (MAD) scaled to give the std for Gaussian distributions. MAD is given by (2) and is a robust alternative statistics to Std. The ROSCO EWS estimate can be found in the file <fst-file-name>.RO.dbg under the name WE_Vw.

$$\text{MAD}(x) = c \text{med}(|x_i - \text{med}(x_i)|) , \quad c = 1.4826 \quad (2)$$

5 Comparing SMPC and "standard" control performance using the OpenFAST 5MW virtual wind turbine

This section uses the SMPC methods from section 3 to produce controller performance results that can be compared to more conventional controllers as the benchmark controller in section 4.

5.1 Simulation software

For the SMPC controllers it is convenient to use the OpenFAST version embedded in MATLAB/Simulink. For this purpose the Simulink/OpenFAST version seen in figure 4 is used. The lower left white boxes are the SMPC pitch and the torque controller. The blue box is the (unsupported) Simulink version of

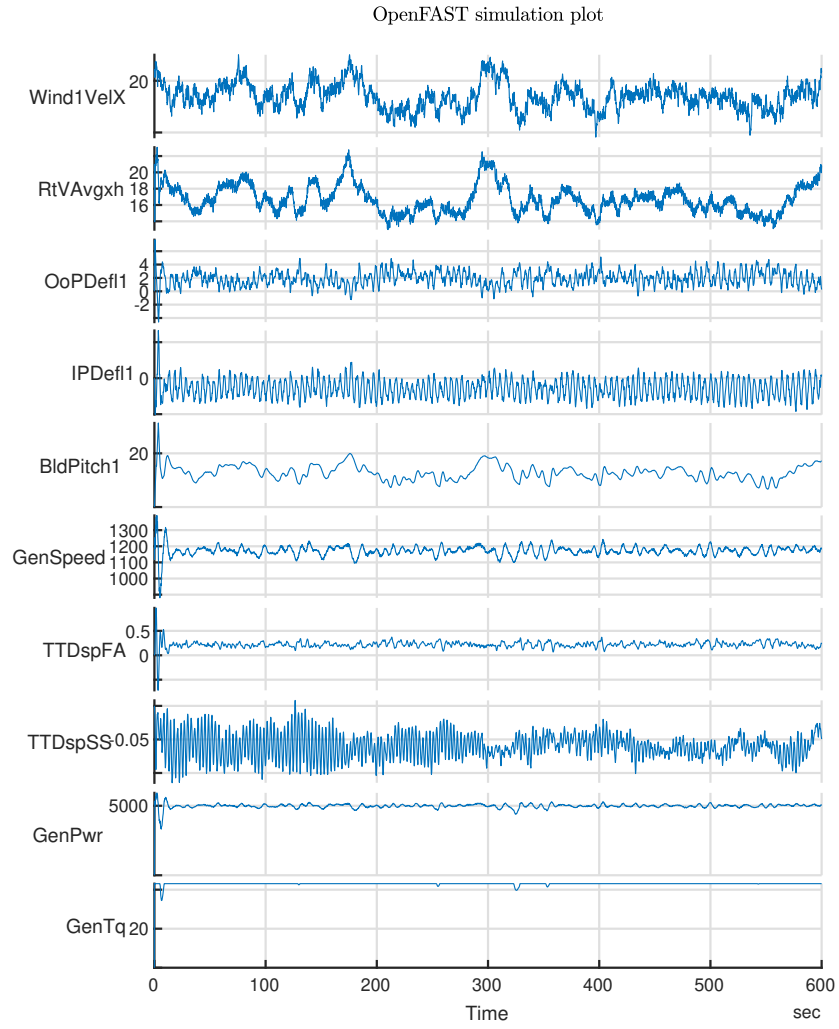


Figure 1: Time plots for the ROSCO controller showing the signals in table 1.

Category	Name	Description	Convention	Units
Wind Motions	Wind1VelX	X component of wind at user selected wind point 1 (Hub height)	Directed along the xi-axis	(m/s)
Rotor	RtVAvgxh	Rotor-disk-averaged relative wind velocity (x-component)	the hub coordinate system	(m/s)
Blade 1 Tip Motions	OoPDefl1	Blade 1 out-of-plane tip deflection (relative to the undeflected position)	Directed along the xc1-axis	(m)
Blade 1 Tip Motions	IPDefl1	Blade 1 in-plane tip deflection (relative to the undeflected position)	Directed along the yc1-axis	(m)
Blade Pitch Motions	BldPitch1	Blade 1 pitch angle (position)	Positive towards feather about the minus zc1- and minus zb1-axes	(deg)
Shaft Motions	GenSpeed	Angular speed of the high-speed shaft and generator	Same sign as LSS-GagVxa/ LSS-GagVxs/ LSSGagV	(rpm)
Tower-Top Motions	TTDspFA	Tower-top fore-aft (translational) deflection (relative to the undeflected position)	Directed along the xt-axis	(m)
Tower-Top Motions	TTDspSS	Tower-top side-to-side (translation) deflection (relative to the undeflected position)	Directed along the yt-axis	(m)
Generator and Torque Control	GenPwr	Electrical generator power	Same sign as GenTq	(kW)
Generator and Torque Control	GenTq	Electrical generator torque	Positive reflects power extracted and negative represents a motoring-up situation (power input)	(kN-m)

Table 1: Signal descriptions taken from OpenFAST documentation (OutListParameters.xlsx).

Names	Mean	Std	CV	Min	Max	DELProxy
Wind1VelX	16.934	2.5623	0.15131	9.096	25.03	NaN
RtVAvgxh	16.639	1.7239	0.1036	12.98	22.77	NaN
OoPDefl1	1.9349	1.0603	0.54802	-1.256	5.138	6.9184
IPDefl1	-0.56868	0.50697	-0.89148	-1.849	0.8826	2.9201
BldPitch1	12.745	2.6167	0.20532	6.627	19.96	332.09
GenSpeed	1172.8	23.827	0.020317	1095	1243	NaN
TTDspFA	0.22089	0.049077	0.22218	0.06567	0.3734	0.49853
TTDspSS	-0.060328	0.01754	-0.29074	-0.1095	0.00818	0.19598
GenPwr	4991.9	111.24	0.022283	4395	5296	NaN
GenTq	43.054	0.27802	0.0064575	39.67	43.09	NaN

Table 2: Main statistics for the chosen signals. The initial first minute is not included. Notice that the number in row DEL for blade pitch is the total traveled angle which is a proxy for wear on the pitch system. The NaN indicates DEL is not relevant for the signal.

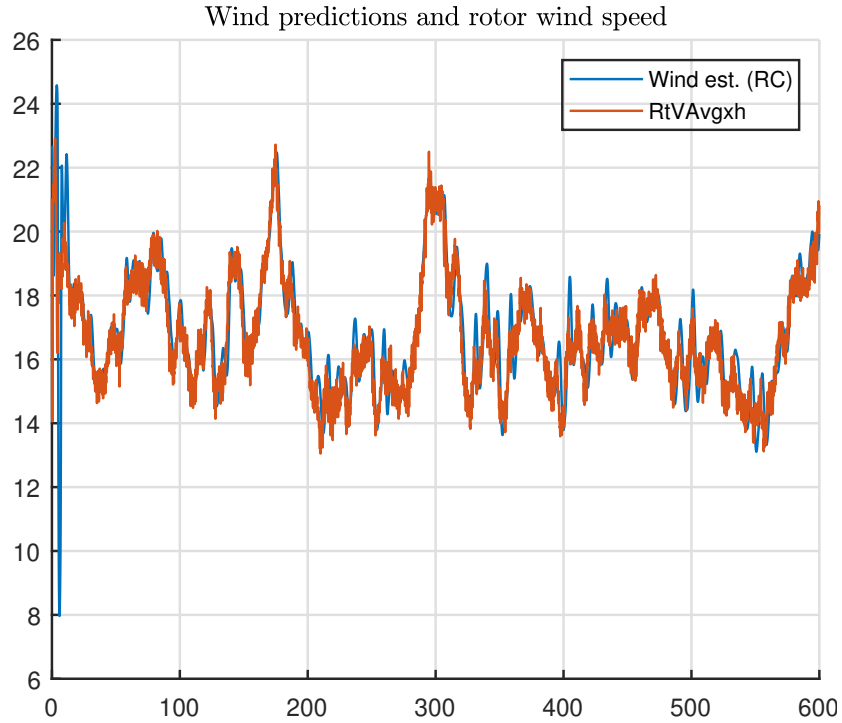


Figure 2: Wind prediction from OpenFAST/ROSCO compared to the EWS proxy RtVAvgxh.

Statistic	WE_Vw-RtVAvgxh	WE_Vw-Wind1VelX
RMS	0.65625	1.704
Mean	0.12091	-0.17471
Std	0.68116	1.7878
MAD scaled	0.62818	1.6836

Table 3: Statistics for the wind estimation error. The initial first minute is not included.

The performance of a WT includes many measures. The main important measures selected here are:

- Probability of violating constraint on speed.
- Pitch activity.
- Tower fatigue.
- Blade fatigue.

The methods to be compared will cover:

- SMPC-OC with only constraint.
- SMPC without constraint but only with penalty on speed (SMPC-OP).
- SMPC with alternative specifications as e.g. penalty on tower movements.
- ROSCO as a *benchmark* controller

It is crucial to at least relate the results obtained with the new SMPC methods to a established proven controller. Just as the used virtual turbine NREL5MW Jonkman et al. [2009] is established as a standard simulation turbine and OpenFAST Jonkman et al. [2009] is accepted as a reliable WT simulation tool, ROSCO is accepted as a good modern WT controller which can be used as a benchmark.

5.3 Operational conditions

In this first investigation of the new SMPC method it is most rational to focus on ambient wind conditions where the difference to other controllers will be most pronounced. The following initial operational conditions is therefore selected:

- Full load (FL) is assumed i.e. wind speeds in the interval 11.4 m/s-25 m/s.
- Start by using 17m/s mean wind which will probably keep the turbine in FL during the whole simulation.
- Constant power generator torque controller as the Kalman filter (KF) is designed for.
- Class B turbulence Commission [2005] is used.
- The ambient mean wind direction is constant.
- The ambient mean wind is constant in each simulation test of e.g. 10 min.

5.4 Controller configuration

The inputs and outputs assumed for the controller must be comparable with the benchmark controller. Also it is necessary to state if the signals are standard for commercial WT or new signals to be explored. In the following the signals are all available on standard commercial WT of horizontal axis pitch and generator controller type which means almost all newer turbines.

The controller configuration is listed below:

- Controller inputs are:
 - Generator speed.
 - Tower accelerations.
- Controller outputs are:
 - Collective pitch.
 - Generator torque.
- Generator torque is handled by constant power control.
- The SMPC controller only handle the pitch.
- Control design model based on physics:
 - Rotational state plus mean and turbulence wind model.
 - Above plus tower fore aft degree of freedom (DOF).
- Hard limits for pitch: 0-90 deg.

Of course there exists other possible controller configuration. Some comments to the above list are therefore in place. All WT has a nacelle anemometer of some kind so it is possible to use this measurement. It is however very disturbed by the rotor and affected by not only the *effective wind speed* but also the pitching. If used it must be assigned a very large uncertainty. For that reason it is not included here. Neither the ROSCO controller uses nacelle measured wind speed for the control. Modern WT has individual pitch but this will not be included here. A simple way to control the generator in FL is to use constant torque or constant power. For the constraint only SMPC-OC controller there is no guaranty that the average speed is at the nominal value. If this is combined with using constant generator torque the power is also not guarantied to be a the nominal value. Using constant power is a easy way to provide nominal power on the average.

5.5 Results for the model in the paper with only speed and wind states and speed constraints

This subsection shows a number of results similar to the ones in section 4. The controller used is the SMPC-OC from the paper Knudsen et al. [2025] where only probability constraint for the generator speed is used. The assessment of the KF goes first as this is crucial for the SMPC to work well.

5.5.1 Tuning of the KF

The KF consist of the dynamic state space (SS) model with parameters that comes from first principles and then the measurement model that have one parameter which is the measurement error variance. In the investigation in the paper both the simulation model and the design model where the same. The KF was based on the same model as generated the data. Here the std on measurement noise was set to 1% of the nominal speed. In reality this number might be smaller. OpenFAST/ROSCO does not add any measurement noise to the speed signal so the KF gets a perfect speed measurement. This is not realistic. A assumed speed uncertainty must be related to the speed variation. In table 2 the coefficient of variation (CV) is 0.022. The relative speed STD must be significantly smaller than this. In this investigation 0.001 is used as the STD for speed measurement noise relative to the nominal speed.

This uncertainty could also be used for the measurement model the KF is based on. However, the OpenFAST simulations model has much more DOFs compared to the design model for the KF. It is therefore expected that some extra uncertainty is needed to account for the model mismatch. In this tuning all extra uncertainty is accommodated for by increasing the measurement variance parameter R . A good choice was found to correspond to a std at 0.03 of the nominal speed which is 30 times higher compared to the measurement noise.

5.5.2 Assessment of the KF

If a residual test can exclude that the one step output prediction errors are white noise the model which the KF is based on is not perfect so there are potential model improvements to do. Even if this is the case the model can be sufficient for its purpose. To assess this the state estimates will be analyzed. In particular the estimate of effective wind is important. It can be compared to the most suitable signal from OpenFAST. The root mean square error (MSE) between these will be calculated and compared to the similar signal using the ROSCO effective wind speed estimator.

The residual analysis is shown in figure 5. The Portmanteau test for white noise residuals has a p-value at 0 so the residuals is not at all white which is also clear from viewing the autocorrelation function in the figure which show a low frequent signal which is also seen in the spectrum. The spectrum also have two small peaks one at 0.6 Hz which probably is the 3P frequency at 0.605 and another one at approximately 1.66 Hz which only match *2nd Blade Asymmetric Flapwise Yaw* calculated by ADAMS [Jonkman et al., 2009, Table 9-1]. From both the time and normal probability plot it is also clear that the residuals has longer tails corresponding to a normal distribution.

All this indicates that there is much potential for improving the model. This is not surprising as the model is as simple as can be without both tower and blade degrees of freedom (DOF).

The one step predictions of the four states relative to the operational point is seen in the top of figure 6. Notice that the last fourth state is the pitch which is necessary as the change in pitch is the control input. Clearly the pitch is not smooth. It either is constant or changes abruptly. The blue wind prediction signal shown in the bottom part of figure 6 shows that the estimate follows the EWS proxy quit well even though it seems to be underestimating the wind speed. The KF used here and the one used in ROSCO can also be expected to perform a like as they both are based on the same model originally described in Knudsen et al. [2011].

Table 4 shows the statistical assessment of the KF. The first column is for the residuals i.e. $\omega(t) - \hat{\omega}(t|t-1)$. The right most two columns are similar to the two columns in table 3 for the ROSCO controller. For the SS model used the total wind prediction is the sum of the second and third state which is the turbulence and slow component of the wind (3). The RMS for the wind state error is $(0.7297/0.65625 = 1.1119)$ slightly larger for the SMPC-OC controller compared to the ROSCO controller. The abrupt pitch signal could perhaps explain some of the difference. The negative (-0.23488) mean wind prediction error also shows the underestimation.

$$\hat{w}(t|t-1) = \hat{x}_2(t|t-1) + \hat{x}_3(t|t-1) \quad (3)$$

5.5.3 Assessment of the controller performance

Using the methods in section II-D in the paper the conditional probability was found to 0.6 to get a unconditional probability of 0.89, which is sufficiently close to the target 0.9, of not exceeding 10% over

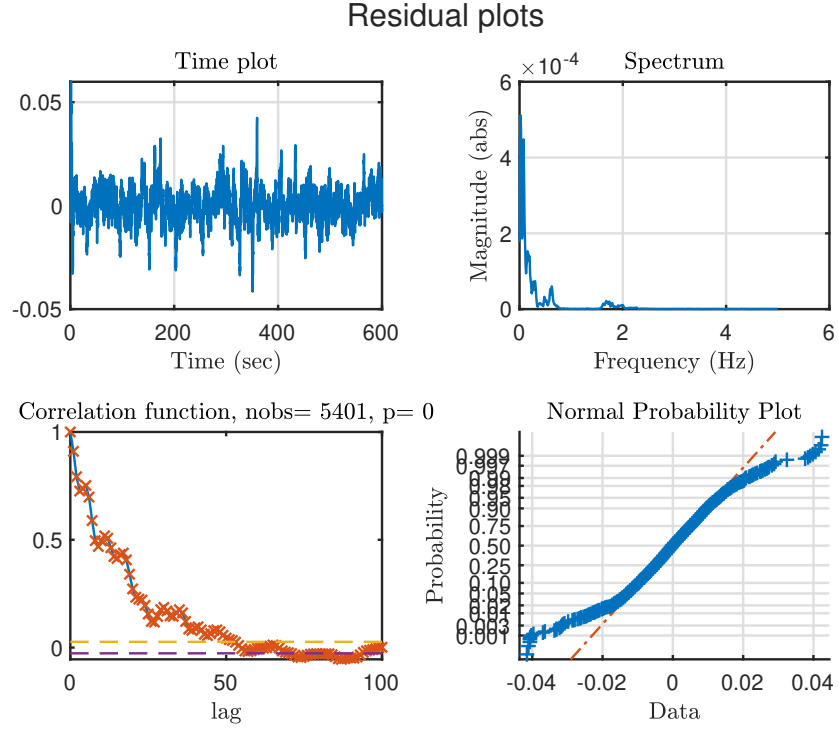


Figure 5: Residual analysis for the KF used in the OpenFAST/SMPC-OC controller.

Statistics	Residuals	$\hat{w}(t t-1)$ -RtVAvgxhR	$\hat{w}(t t-1)$ -Wind1VelXR
RMS	0.0083506	0.7297	1.8089
Mean	-9.3846e-05	-0.23488	-0.5293
Std	0.0083508	0.69093	1.7299
MADScaled	0.007408	0.6712	1.7152

Table 4: Statistics for the residual and wind prediction error using the SMPC-OC controller with constraints only. The initial first minute is not included.

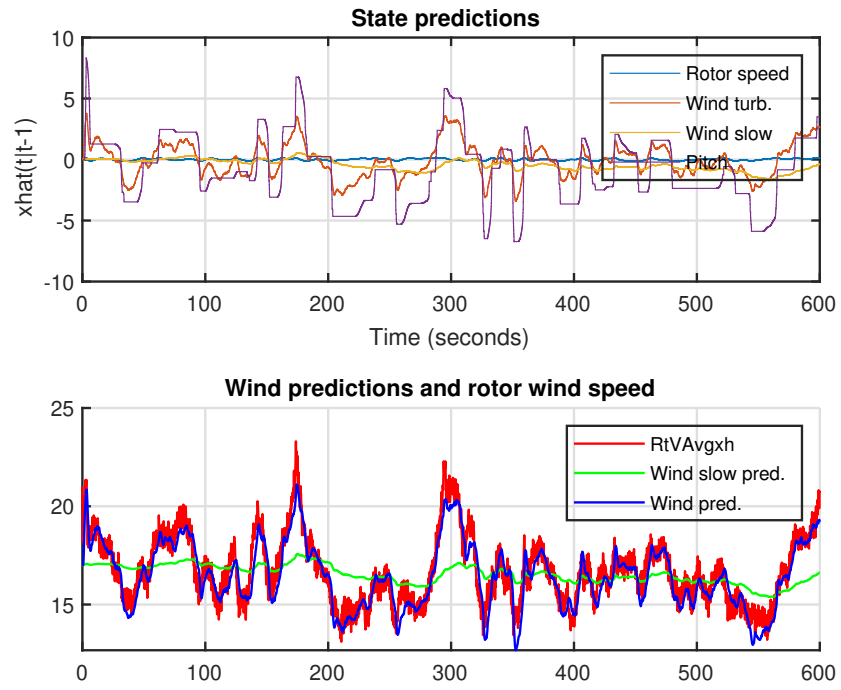


Figure 6: Top: One step state predictions relative to the operational point. Bottom: Wind prediction from OpenFAST/SMPC-OC compared to the EWS proxy RtVAvgxh. Legend: blue is total wind, green is the slow wind part.

or under-speed. For this controller OpenFAST/Simulink has produced 10 min. of simulation that gives the below results similar to figure 1 and table 2.

Figure 7 shows both the SMPC-OC controller performance and the ROSCO for reference. As seen the ambient wind $Wind1VelX$ is exactly the same for both controllers but the $RtVAvgxh$ is slightly different as this is the relative rotor average wind and the rotor movements are different for the two controllers. The immediate visual impression is that the SMPC-OC controller is inferior to ROSCO as the tower fore-aft (TTDspFA) moves more. Most other fatigue related movement are more similar between the controllers. Also the allowed speed variation is much larger for the SMPC-OC controller. The basic potential for this SMPC-OC controller with only constraints on the speed is to have low fatigue while the pitch is constant. To investigate this further the shaded areas mark the time intervals where the SMPC-OC controller only changes pitch within 0.1 degrees in at least 10 seconds. To focus more figure 8 shows only selected signals. It is evident that the movement of especially the tower TTDspFA for SMPC-OC is smaller in the shaded areas compared to the non shaded. Also, in the shaded areas the tower TTDspFA is maybe even smaller for SMPC-OC compared to ROSCO. This shows that the basic idea for this controller seems to work.

To do the assessment numerically table 5 has been produced. Most of the relative values in the bottom half of table 5 except the means should be low. Clearly the SMPC controller is inferior as all the fatigue related numbers but $BldPitch1$ are above 1. The blade and tower fatigue are between 6 and 53% larger for SMPC-OC compared to ROSCO. The pitch total travel is only 52% smaller but then again this is explained by the larger speed variation. The visual inspection could suggest SMPC-OC is better than ROSCO for e.g. TTDspFA in some of the shaded areas but even in that case this is all lost due to the abrupt pitching outside the shaded areas.

5.6 Results for the model in the paper with only speed and wind states and speed penalty

This subsection shows a number of results similar to the ones in section 4 and 5.5. The controller used is the SMPC-OP from the paper Knudsen et al. [2025] where only penalty on generator speed is used but no constraint for the generator speed is used. This means that the penalty matrix in (4) S_i , which was 0 for the SMPC-CO will now have a positive value in the upper left corner corresponding to the speed state. This value is increased from a low value until the speed 10% limit is obtained 90% of the time. The penalty on pitch changes T_i is fixed to 1 as for the SMPC-CO.

$$V_k = \sum_{i=H_w}^{H_p} (\hat{x}_{k+i|k} - r_{k+i})^T S_i (\hat{x}_{k+i|k} - r_{k+i}) + \sum_{i=0}^{H_u-1} \Delta u_{k+i}^T T_i \Delta u_{k+i} + c \quad (4)$$

5.6.1 Assessment of the KF

As the physical model used for the KF has not changed the KF is not re-tuned. Figure 9 10 and table 6 shows results similar to the ones in section 5.6.1.

The residuals in figure 9 is more Gaussian compared to the ones with only constraints in figure 5. Further, table 6 shows that the RMS on residuals and the error for EWS is slightly smaller compared to table 4 for the constraints only SMPC-OC controller. This supports the hypothesis that the KF performance is decreased for more abrupt pitch changes.

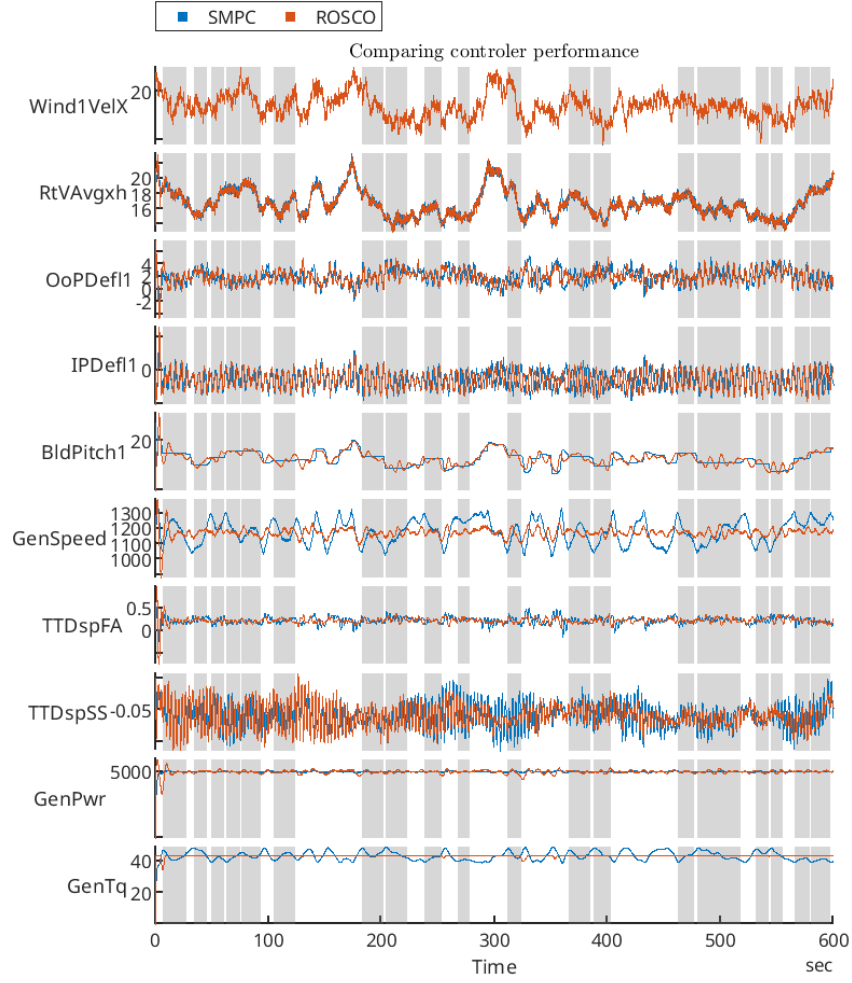


Figure 7: Time plots for the SMPC-OC controller showing the signals in table 1. Legends: Blue: SMPC-OC controller, red: ROSCO controller. The shaded areas mark the time intervals where the SMPC-OC controller only changes pitch within 0.1 degrees in at least 10 seconds.

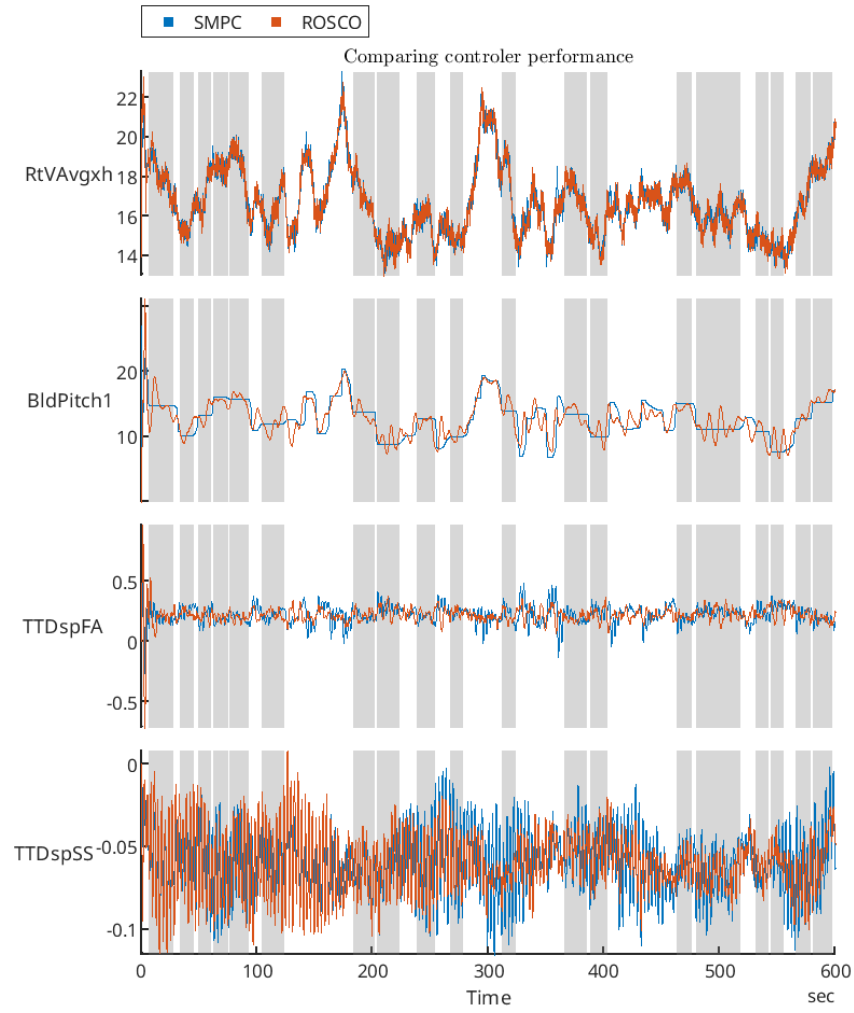


Figure 8: Time plots for the SMPC-OC controller focusing on tower movements. Otherwise similar to figure 7.

Names	Mean	Std	CV	Min	Max	DELProxy
Values for SMPC-OC						
Wind1VelX	16.934	2.5623	0.15131	9.0957	25.03	NaN
RtVAvgxh	16.64	1.7291	0.10391	13.105	23.304	NaN
OoPDefl1	1.9653	1.1664	0.5935	-1.9559	5.1801	7.3689
IPDefl1	-0.56916	0.51868	-0.91131	-1.8047	1.1418	3.1655
BldPitch1	12.659	2.7744	0.21916	6.8059	20.359	157.74
GenSpeed	1176.7	75.895	0.064497	1015.3	1334.3	NaN
TTDspFA	0.22202	0.070815	0.31896	-0.13508	0.48111	0.76107
TTDspSS	-0.060333	0.019846	-0.32894	-0.11539	-0.0019257	0.21313
GenPwr	5001.3	35.988	0.0071958	4894	5114.6	NaN
GenTq	43.167	2.7268	0.063169	38.727	49.046	NaN
Values for SMPC-OC relative to ROSCO						
Wind1VelX	1	1	1	0.99997	0.99999	NaN
RtVAvgxh	1.0001	1.003	1.003	1.0096	1.0235	NaN
OoPDefl1	1.0157	1.1	1.083	1.5573	1.0082	1.0651
IPDefl1	1.0008	1.0231	1.0222	0.97603	1.2937	1.0841
BldPitch1	0.99328	1.0602	1.0674	1.027	1.02	0.475
GenSpeed	1.0034	3.1852	3.1745	0.92719	1.0734	NaN
TTDspFA	1.0051	1.4429	1.4356	-2.057	1.2885	1.5266
TTDspSS	1.0001	1.1315	1.1314	1.0538	-0.23541	1.0875
GenPwr	1.0019	0.32354	0.32293	1.1135	0.96575	NaN
GenTq	1.0026	9.8079	9.7822	0.97623	1.1382	NaN

Table 5: Main statistics for the chosen signals using the SMPC-OC controller. The initial first minute is not included. Notice that the number in row DEL for blade pitch is the total traveled angle which is a proxy for wear on the pitch system. The NaN indicates DEL is not relevant for the signal.

Statistics	Residuals	$\hat{w}(t t-1)$ -RtVAvgxhR	$\hat{w}(t t-1)$ -Wind1VelXR
RMS	0.007026	0.70428	1.8045
Mean	-0.0001036	-0.251	-0.5463
Std	0.0070259	0.6581	1.72
MADScaled	0.0069098	0.64807	1.7075

Table 6: Statistics for the residual and wind prediction error using the SMPC-OP controller with constraints only. The initial first minute is not included.

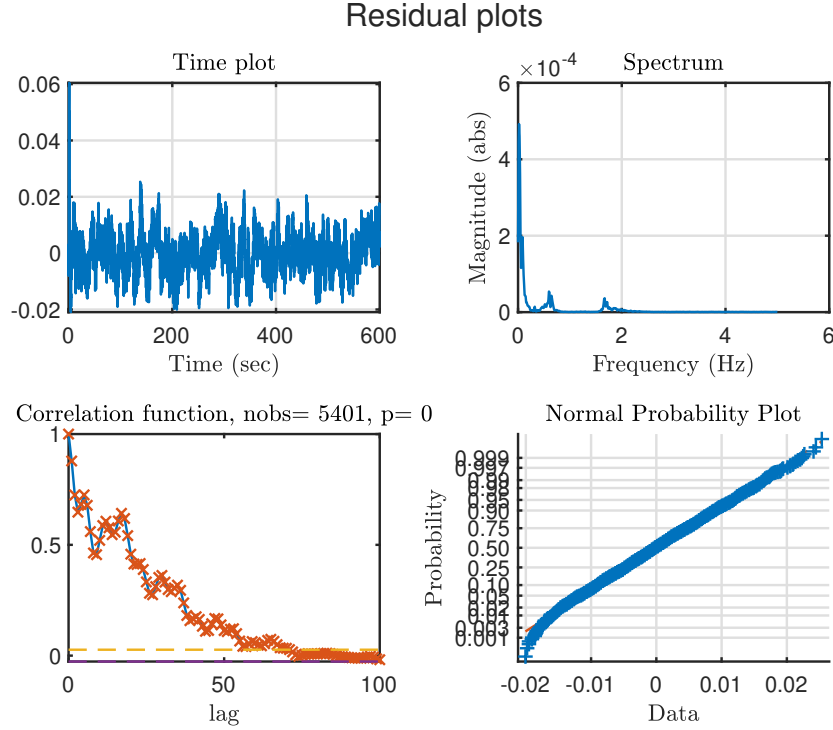


Figure 9: Residual analysis for the KF used in the OpenFAST/SMPC-OP controller.

5.6.2 Assessment of the controller performance

The time plots in figure 11 clearly shows that the speed varies more and more smooth for SMPC-OP compared to ROSCO. Also the pitch is more smooth and low frequent for SMPC-OP.

Table 7 shows the results for SMPC-OP and compares it to ROSCO. In terms of fatigue the SMPC-OP controller is better than ROSCO as the blade fatigue is similar, the traveled pitch is half and the tower fatigue is at least 6.5% smaller. However, this can very well all be explained by the speed std being 3 times larger for SMPC-OP compared to ROSCO. The penalty on speed variations for the SMPC-OP has been increased until the std on speed was the same as for ROSCO and then the fatigue where up to 22% larger compared to ROSCO except for TTDspSS which where 12% smaller. Notice also the example of the difference between std and DEL where the std for TTDspFA has increased 7% for SMPC-OP compared to ROSCO but the DEL has decreased 7.5%. As the SMPC-OP is better regarding fatigue compared to ROSCO it is probably also better than SMPC-CO. To check this table 8 similar to the bottom half of table 7 where numbers for SMPC-OP are related to SMPC-CO is produced and shown in appendix A where it is seen that SMPC-OP are better on all parameters.

6 Conclusion

This deliverable aims at assessing the potential benefits of using SMPC for single turbine control. In high winds the basic idea is to keep the blade pitch more steady to avoid exciting the tower etc. by only pitching when the probability of exceeding generator speed limits becomes to large.

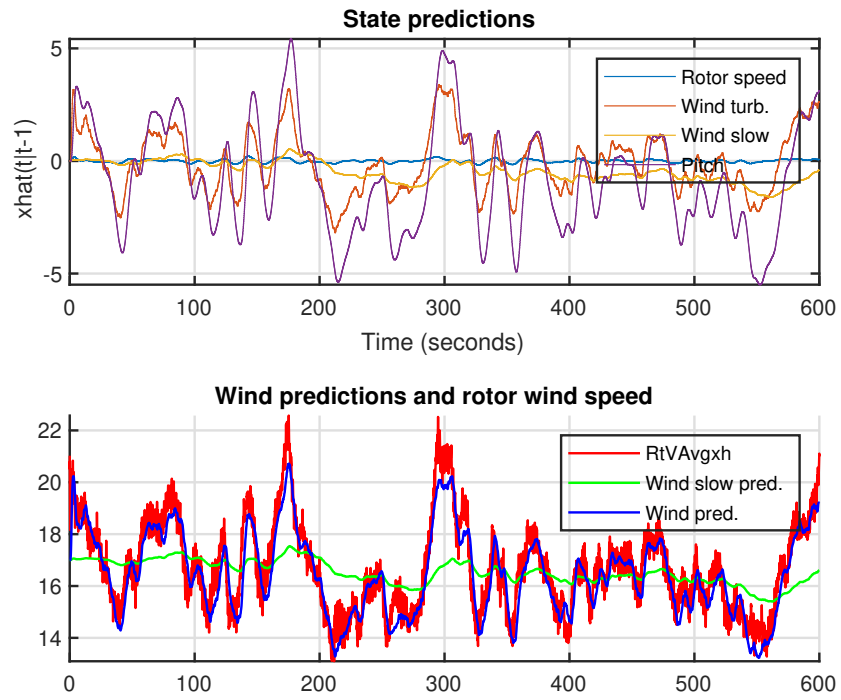


Figure 10: Top: One step state predictions relative to the operational point. Bottom: Wind prediction from OpenFAST/SMPC-OP compared to the EWS proxy $RtVAvgxh$. Legend: blue is total wind, red is the slow wind part.

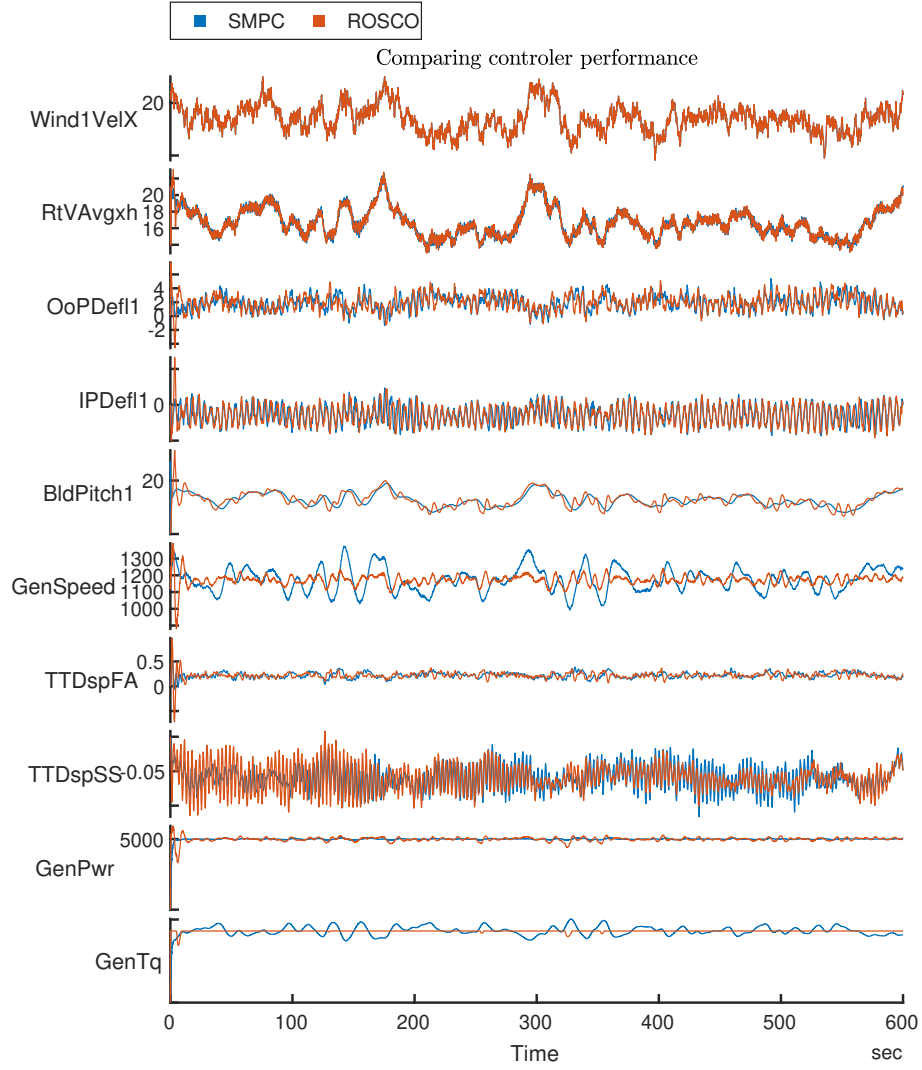


Figure 11: Time plots for the SMPC-OP controller showing the signals in table 1. Legends: Blue: SMPC-OP controller, red: ROSCO controller.

Names	Mean	Std	CV	Min	Max	DELProxy
Values for SMPC-OP						
Wind1VelX	16.934	2.5623	0.15131	9.0957	25.03	NaN
RtVAvgxh	16.639	1.7259	0.10373	13.099	22.572	NaN
OoPDefl1	1.941	1.0881	0.56057	-1.3997	5.4065	6.9642
IPDefl1	-0.57037	0.51632	-0.90523	-1.7409	0.9302	2.9125
BldPitch1	12.663	2.4022	0.1897	8.046	18.957	150.99
GenSpeed	1173.2	71.325	0.060794	992.23	1375.1	NaN
TTDspFA	0.22102	0.052524	0.23765	0.036154	0.3861	0.46095
TTDspSS	-0.060579	0.017207	-0.28405	-0.11597	-0.0066056	0.18318
GenPwr	5000.9	32.208	0.0064405	4907.2	5124.9	NaN
GenTq	43.271	2.559	0.05914	37.16	50.35	NaN
Values for SMPC-OP relative to ROSCO						
Wind1VelX	1	1	1	0.99997	0.99999	NaN
RtVAvgxh	1	1.0012	1.0012	1.0091	0.99131	NaN
OoPDefl1	1.0032	1.0262	1.0229	1.1144	1.0522	1.0066
IPDefl1	1.003	1.0184	1.0154	0.94154	1.0539	0.99742
BldPitch1	0.99356	0.918	0.92395	1.2141	0.94976	0.45467
GenSpeed	1.0004	2.9934	2.9922	0.90615	1.1063	NaN
TTDspFA	1.0006	1.0702	1.0696	0.55055	1.034	0.92461
TTDspSS	1.0042	0.98105	0.97698	1.0591	-0.80753	0.93466
GenPwr	1.0018	0.28955	0.28903	1.1165	0.96769	NaN
GenTq	1.0051	9.2046	9.1583	0.93673	1.1685	NaN

Table 7: Main statistics for the chosen signals using the SMPC-OP controller. The initial first minute is not included. Notice that the number in row DEL for blade pitch is the total traveled angle which is a proxy for wear on the pitch system. The NaN indicates DEL is not relevant for the signal.

The present methods for SMPC has some issues which are solved in the first part of this deliverable. The solution is demonstrated on the simplest possible wind turbine model. This part is documented in a paper which is accepted for presentation at ACC2025.

The second part of the deliverable uses the methods from the first part to develop a SMPC controller but now the assessment is done using the high fidelity simulation software OpenFAST using the NREL5MW turbine. It is of course very important to compare results from new methods to the existing state of art. For this the broadly accepted controller ROSCO is used in a version particularly tuned for NREL5MW.

The EKF can also be compared to the ROSCO controller which also includes a EKF. One problem is though that OpenFAST does not have exactly the EWS signal but a reasonable proxy the $RtVAvgxh$ signal. Comparing using this signal the EKF used here has 11% larger RMSE relative to the EKF in ROSCO. Based on this the EKF is acceptable.

The numerical comparison of SMPC-OC to ROSCO shows that the tower fore aft fatigue increases 53% at the other fatigue less than 10% except the pitch travel which is reduced to 45%. Consequently, a reduction in blade and tower fatigue has not been achieved. However, the visual inspection of time plots shows that the SMPC-OC have reduced tower fore aft movements in the intervals with steady pitch maybe even compared to ROSCO so the fundamental idea behind this seems to hold. The problem is that the large and fast pitch change at the end of a steady period excited the blade and tower so much that this apparently increases fatigue more than it is reduced in the steady periods.

A SMPC-OP has been tuned using only speed penalty but no explicit constraints to achieved the same speed variations as the SMPC-OC. The SMPC-OP is superior to SMPC-OC probably again because it does not have abrupt pitch changes but more smooth pitch behavior. Also the SMPC-OP has up to 7.5% less fatigue compared to ROSCO. This is however because of the 3 times larger speed variation.

7 Future work

This work inspires a number of point for further investigation. Many of them fits nicely into the WP3 task T3.4: Control performance improvement with LIDAR measurements. The main points are listed below.

- For the 4 state model used in this investigation.
 - Test if reducing max pitch speed improves the SMPC-OC performance.
 - Test if combinations of penalty and constraint improves the performance.
- State estimator.
 - Develop a EKF that covers the whole wind speed range.
 - Consider using a UKF in place of the EKF.
- Linearization and gain scheduling.
 - Use the slow wind speed state for finding the linearization (beta,lambda) point.
- Model structure.
 - Include at least the tower fore aft DOF.
 - Include more DOFs as blade and tower side side.

References

- N. J. Abbas, D. S. Zalkind, L. Pao, and A. Wright. A reference open-source controller for fixed and floating offshore wind turbines. *Wind Energy Science*, 7(1):53–73, 2022. doi: 10.5194/wes-7-53-2022. URL <https://wes.copernicus.org/articles/7/53/2022/>.
- I. E. Commission. International standard 61400-1 - wind turbines. Technical report, International Electrotechnical Commission, 2005.
- J. Jonkman, S. Butterfield, W. Musial, and G. Scott. Definition of a 5-mw reference wind turbine for offshore system development. Technical Report NREL/TP-500-38060, National Renewable Energy Laboratory, 1617 Cole Boulevard, Golden, Colorado, USA, 2009.
- T. Knudsen, M. Soltani, and T. Bak. Prediction models for wind speed at turbine locations in a wind farm. *Wind Energy*, 14:877–894, 2011. Published online in Wiley Online Library (wileyonlinelibrary.com). DOI: 10.1002/we.491.
- T. Knudsen, S. Hassani, and R. Wisniewski. Stochastic MPC with focus on probabilistic constraints with application to wind turbine control. In *2025 American Control Conference, July 8 - 10, Denver, Colorado*, pages ?–? AACC, IFAC, 2025. Preprint.

A Comparing SMPC-OP to SMPC-OC

Names	Mean	Std	CV	Min	Max	DELProxy
Values for SMPC-OP relative to SMPC-OC						
WindVelX	1	1	1	1	1	NaN
RtVAvgxh	0.99993	0.99814	0.9982	0.99952	0.96858	NaN
OoPDefl1	0.98764	0.93285	0.94452	0.7156	1.0437	0.94508
IPDefl1	1.0021	0.99545	0.99333	0.96466	0.81466	0.92008
BldPitch1	1.0003	0.86584	0.86559	1.1822	0.93114	0.95721
GenSpeed	0.99703	0.93979	0.94259	0.97731	1.0306	NaN
TTDspFA	0.99549	0.74171	0.74507	-0.26765	0.80251	0.60566
TTDspSS	1.0041	0.86705	0.86353	1.005	3.4303	0.85945
GenPwr	0.99993	0.89496	0.89503	1.0027	1.002	NaN
GenTq	1.0024	0.93848	0.93621	0.95953	1.0266	NaN

Table 8: Main statistics for the chosen signals using the SMPC-OP controller. The initial first minute is not included. Notice that the number in row DEL for blade pitch is the total traveled angle which is a proxy for wear on the pitch system. The NaN indicates DEL is not relevant for the signal.

Stochastic MPC with focus on probabilistic constraints with application to wind turbine control

Torben Knudsen and Sina Hassani and Rafal Wisniewski

Abstract—The literature on stochastic MPC (SMPC) claims probabilistic constraints give a major feasibility problem and suggest solutions based on a combination of feedback and MPC. This paper explains it makes sense to relax the probabilistic constraints after the first part of the prediction horizon which solves the feasibility problem. Further, it is demonstrated that the effect that is special to probabilistic constraints is that they change the distribution of inputs and outputs. Current SMPC uses the *conditional constraint probability given current measurements* as the design parameter. Here a method to relate to the more application relevant *unconditional constraint probability* is developed. Finally, all the points are demonstrated with a simple wind turbine control problem which served as the motivation for this research in the first place.

I. INTRODUCTION

This research was motivated by an idea from wind turbine (WT) control [2]. The most important control objective in single WT control is to keep the rotational speed right which depends on average wind speed [3, Chap. 8] [4, Chap. 4]. When the average wind speed is sufficient to produce nominal generator power the rotational speed is controlled by blade pitching. The objective is to keep the rotational speed within approximately $\pm 10\%$ of nominal rotational speed where the specific limits depend on the turbine, 20% is specified for the IEA-22MW reference wind turbine [5]. The most costly violation of the rotational speed constraints is over speeding which initiates an emergency shut down with large mechanical loads in blade and tower as a result. The common solution is to tune a PI controller to follow a rotational speed set point sufficiently close to keep the rotational speed within the limits. Other control design methods as LQG [6] and MPC [7] has been investigated but still with the objective of set point following [4, Chap. 4.1.4].

The new idea is to completely abandon speed *set point following* but only focus on *staying within speed limits* with a high probability. The hypothesized advantage is that the pitch would be constant in small time intervals which would reduce the average fatigue load compared to the traditional method. The most straightforward approach would be Stochastic Model Predictive Control (SMPC), where a cost is applied to pitch actuation, and the rotational speed error is subject only to probabilistic constraints without any associated cost.

This work was supported by the European Union project ICONIC 101122329

All authors are with Automation and Control, Department of Electronic Systems, Aalborg University, Denmark {tk, sinah, raf}@es.aau.dk

Initial investigation and literature study in this area with focus on constraints in SMPC lead to the following general questions:

- 1) How to avoid the prediction variance increasing so much that the problem becomes infeasible for longer prediction horizons?
- 2) How does SMPC with *explicit constraints* compare to SMPC/MPC/LQG with out constraints but where the same constraints behavior is obtained by tuning costs? The latter approach can be called *implicit constraint*.
- 3) The important probability in applications is the *unconditional* probability of violating constraints but the existing SMPC methods use the *conditional* probability given the measurements up to the current time. Can a specified unconditional probability be obtain by tuning the conditional probability?

Especially the first question is discussed in the literature. In [8] it is stated that "open loop control" used in MPC gives conditional state variance which evolves in an "uncontrolled fashion" which may "induce serious feasibility problems". The suggested solution to this is to introduce a kind of feedback called "disturbance feedback control" (see [8] for more details). This solution is also suggested by several other papers [9], [10], [11], [12].

The literature studied has not offered any insight to the second question.

The third question on how to specify the probability constraints in a application relevant way is also mostly missing in the literature. [11] suggests to use either the conditional mean state estimate or the conditional probability of state violations but seems to leave the choice to the user.

Consequently, these questions seems largely uncovered in the literature. The contribution of this paper is the investigation of these problems and suggestions for solutions.

The remaining part of the paper first introduces the SMPC problem for linear systems and analyzes the three questions and suggest possible solutions. Then the questions and solutions are illustrated and accessed using simulation of a very simplified WT speed control problem. Finally, some conclusions are drawn.

II. SMPC PROBLEM FORMULATION AND CHALLENGES

The model used for the SMPC is the standard Markov state space (SS) model (1)

$$x_{k+1} = Ax_k + Bu_k + w_k, \quad w_k \sim \text{NID}(\underline{0}, Q), \quad (1a)$$

$$y_k = Cx_k + v_k, \quad v_k \sim \text{NID}(\underline{0}, R), \quad (1b)$$

$$E(w_k v_l^T) = \underline{0}, \quad (1c)$$

where $\sim \text{NID}(\mathbf{0}, W)$ stand for Normal Independent Distributed with covariance W , i.e., Gaussian white noise.

A. Cost function

The cost function V_k (2) is the mean value of the standard deterministic MPC cost. It is based on x to simplify and as this also covers the often used “output” $z = C_z x$.

$$V_k = E_k \left(\sum_{i=H_w}^{H_p} (x_{k+i} - r_{k+i})^T S_i (x_{k+i} - r_{k+i}) \right) + \sum_{i=0}^{H_u-1} \Delta u_{k+i}^T T_i \Delta u_{k+i} \quad (2a)$$

$$\mathcal{Y}_k \triangleq y_0, y_1, y_2 \dots y_k, u_0, u_1, u_2 \dots u_k \quad (2b)$$

$$E_k(\bullet) \triangleq E(\bullet | \mathcal{Y}_k) \quad (2c)$$

$$\Delta u_{k+i} = u_{k+i} - u_{k+i-1}, \Delta u_{k+i} = 0 \text{ for } i \geq H_u, \quad (2d)$$

$$S_i > 0, T_i \geq 0 \quad (2e)$$

$$H_p \geq H_w > 0, H_p \geq H_u \quad (2f)$$

Notice that the input is deterministic as it is the decision variable to be found by the SMPC control method to be designed. The conditional expectation given current measurements (2b) in (2a) is needed as x is a stochastic process. Expectation of general functions can only be approximated by e.g. the scenario [13] or the unscented method [14]. However in the case of a quadratic function the expectation can exploit the outcome of a Kalman filter (KF).

Given measurements and initial values (3a) the KF can calculate the estimate (3b) that minimizes the squared norm of the error (3c) such that the error becomes independent of the estimate (3e). The KF also gives the state error covariance $P_{k+j|k} = E(\tilde{x}_{k+j|k} \tilde{x}_{k+j|k}^T) \quad (3d)$.

$$x_0 \sim N(\hat{x}_0, P_0) \quad (3a)$$

$$\hat{x}_{k+j|k} = E(x_{k+j} | \mathcal{Y}_k), \quad (3b)$$

$$\tilde{x}_{k+j|k} \triangleq x_{k+j} - \hat{x}_{k+j|k}, \quad (3c)$$

$$\tilde{x}_{k+j|k} \sim N(\mathbf{0}, P_{k+j|k}), \quad (3d)$$

$$\tilde{x}_{k+j|k}, \hat{x}_{k+j|k} \text{ are independent} \quad (3e)$$

Using (3) the SMPC cost function (2a) can be turned into a usable quadratic cost function similar to the MPC. For one i in (2a) the expectation can be calculated as (4).

$$\begin{aligned} & E_k \left((x_{k+i} - r_{k+i})^T S_i (x_{k+i} - r_{k+i}) \right) \\ &= E_k \left((\tilde{x}_{k+i|k} + \hat{x}_{k+i|k} - r_{k+i})^T S_i (\tilde{x}_{k+i|k} + \hat{x}_{k+i|k} - r_{k+i}) \right) \\ &= (\hat{x}_{k+i|k} - r_{k+i})^T S_i (\hat{x}_{k+i|k} - r_{k+i}) \\ &\quad + E_k \left(\tilde{x}_{k+i|k}^T S_i (\hat{x}_{k+i|k} - r_{k+i}) \right) \\ &\quad + E_k \left((\hat{x}_{k+i|k} - r_{k+i})^T S_i \tilde{x}_{k+i|k} \right) \\ &\quad + E_k \left(\tilde{x}_{k+i|k}^T S_i \tilde{x}_{k+i|k} \right) \\ &= (\hat{x}_{k+i|k} - r_{k+i})^T S_i (\hat{x}_{k+i|k} - r_{k+i}) \\ &\quad + \text{trace}(S_i P_{k+i|k}) \end{aligned} \quad (4)$$

Notice that $\text{trace}(S_i P_{k+i|k})$ does not depend on u only $\hat{x}_{k+i|k}$ does. This results in the deterministic MPC cost function (5) where c does not depend on u .

$$V_k = \sum_{i=H_w}^{H_p} (\hat{x}_{k+i|k} - r_{k+i})^T S_i (\hat{x}_{k+i|k} - r_{k+i}) + \sum_{i=0}^{H_u-1} \Delta u_{k+i}^T T_i \Delta u_{k+i} + c \quad (5)$$

This turns the SMPC cost function (2a) into the standard MPC cost function (5).

B. Probability constraints

In the deterministic setting there are constraints on the input changes (6a) and the states (6b). Constraints on the input and output can also be useful but this is not relevant for the discussion here.

$$G \Delta u_{k+i} \leq g_i, i = 0, \dots, H_u - 1 \quad (6a)$$

$$F x_{k+i} \leq f_i, i = H_w, \dots, H_p \quad (6b)$$

The constraints on the input is unchanged in the stochastic case.

The constraints on the stochastic state can however only be obtained with some probability. From an application point of view the most relevant probabilistic constraint would normally be (7) i.e. the constraint must be enforced with a high *unconditional* probability p which would mean that the limits will be met a fraction p of the time on the average.

$$P(F x_k \leq f) \geq p \quad (7)$$

As the constraint (7) is intractable the pursuit of a practical approximation starts from (6b).

The most straight forward probabilistic formulation of (6b) would be (8) where p typically would be close to 1 e.g. 0.99.

$$P \left(\bigcap_{i=H_w}^{H_p} F x_{k+i} \leq f_i \right) \geq p \quad (8)$$

The system (1) is linear with Gaussian input so if the controller also is linear in the output all states and output would be Gaussian and the probability (8) could be calculated. However, in general where there are active constraints the controller is not linear and the Gaussianity can not be assumed so the probability (8) can not be calculated in a closed form.

If the constraint is based on the conditional probability of violation given current measurements (9) it is possible to calculate it as all the future states are Gaussian with a conditional mean and covariance given by the KF where the necessary future inputs of course must be known.

$$P \left(\bigcap_{i=H_w}^{H_p} F x_{k+i} \leq f_i | \mathcal{Y}_k \right) \geq p \quad (9)$$

Using $x_{k+i} = \hat{x}_{k+i|k} + \tilde{x}_{k+i|k}$ it can be established [15] that (9) is a convex set for $\hat{x}_{k+i|k}$ and consequently for the input.

Even though this constraint does not spoil the convexity of the problem it will be useful to turn it into something similar to the MPC form (6b) consisting of linear constraints for $\hat{x}_{k+i|k}$. An approximation for this can be obtained using the unscented transform [14].

The common way to obtain linear constraints is however to split (9) up into scalar constraints (10)

$$\begin{aligned} P(F_r x_{k+i} \leq f_{i_r} | \mathcal{Y}_k) &\geq p_{i_r}, \\ i &= H_w, \dots, H_p, \quad r = 1, \dots, n_r \end{aligned} \quad (10)$$

where F_r is row r in F with n_r rows and f_{i_r} is component r in f_i . As shown in [8] using Boole's inequality the condition (11) results in (10) implying (9).

$$\sum_{i=H_w}^{H_p} \sum_{r=1}^{n_r} (1 - p_{i_r}) = 1 - p \quad (11)$$

This is however a very conservative approximation for (9) which is anyway far from (8) which is the application relevant probability. Therefore it is more common to consider p_{i_r} as tuning parameters which are also often chosen equal [8], [9], [11].

[8] considers the unconditional joint constraints probability (8) initially but without any arguments uses the scalar conditional constraints (10). [9] uses the conditional scalar constraints (10) because joint constraints (8) are "nonconvex" which is true in general but not for Gaussian distributions [15]. [11] uses the conditional scalar constraints (10) without any arguments but mentions unconditional joint constraints probability as a challenge for future research. Also [12] uses the conditional scalar constraints (10) without any arguments. To summarize, the literature suggest to use the conditional scalar linear probability constraints because it is mathematical convenient but seems to forget the unconditional probability constraints are more application relevant.

The change from the *unconditional joint* probability constraint (8) to the *conditional individual scalar* constraints (10) involves two steps, from joint to individual and from unconditional to conditional. The former is given more attention in the literature even though the latter is as important. At least it is important to understand the relation between the conditional and unconditional probability of exceeding the constraint. This will depend very much on the system and nothing exacts can be said about it. However, the two probabilities are related through (12a).

$$\begin{aligned} P(F_r x_{k+i} > f_{i_r}) \\ = \int_{\mathcal{Y}_k} P(F_r x_{k+i} > f_{i_r} | \mathcal{Y}_k) p(\mathcal{Y}_k) d\mathcal{Y}_k \end{aligned} \Rightarrow \quad (12a)$$

$$\begin{aligned} P(F_r x_{k+i} > f_{i_r} | \mathcal{Y}_k) &\leq 1 - p_{i_r} \\ \Rightarrow P(F_r x_{k+i} > f_{i_r}) &\leq 1 - p_{i_r} \end{aligned} \quad (12b)$$

This shows that if the maximum conditional constraint violation probability is $1 - p_{i_r}$ so is the unconditional as it is the mean value of the conditional. However, normally the unconditional violation probability will be far smaller than the conditional as demonstrated in section III.

C. The feasibility problem

Consider the conditional scalar constraint (10) for some i, r . Exploring the Gaussianity (13a) the constraint probability can be calculated by (13b) where ϕ is the CDF for the $N(0, 1)$ distribution.

$$x_{k+i} | \mathcal{Y}_k \sim N(\hat{x}_{k+i|k}, P_{k+i|k}) \Rightarrow \quad (13a)$$

$$\begin{aligned} P(F_r x_{k+i} \leq f_{i_r} | \mathcal{Y}_k) \\ = P\left(\frac{F_r x_{k+i} - F_r \hat{x}_{k+i|k}}{\sqrt{F_r P_{k+i|k} F_r^T}} \leq \frac{f_{i_r} - F_r \hat{x}_{k+i|k}}{\sqrt{F_r P_{k+i|k} F_r^T}}\right) \\ = \phi\left(\frac{f_{i_r} - F_r \hat{x}_{k+i|k}}{\sqrt{F_r P_{k+i|k} F_r^T}}\right) \end{aligned} \quad (13b)$$

The probabilistic constraint can then be turned into the standard linear MPC constraint (14d).

$$P(F_r x_{k+i} \leq f_{i_r} | \mathcal{Y}_k) \geq p_{i_r} \Rightarrow \quad (14a)$$

$$\phi\left(\frac{f_{i_r} - F_r \hat{x}_{k+i|k}}{\sqrt{F_r P_{k+i|k} F_r^T}}\right) \geq p_{i_r} \Rightarrow \quad (14b)$$

$$\frac{f_{i_r} - F_r \hat{x}_{k+i|k}}{\sqrt{F_r P_{k+i|k} F_r^T}} \geq \phi^{-1}(p_{i_r}) \Rightarrow \quad (14c)$$

$$F_r \hat{x}_{k+i|k} \leq f_{i_r} - \phi^{-1}(p_{i_r}) \sqrt{F_r P_{k+i|k} F_r^T} \quad (14d)$$

Notice that if $p_{i_r} = \frac{1}{2}$ then the last term in (14d) will be zero and the constraint will be for the conditional mean state but if $p_{i_r} > \frac{1}{2}$ e.g. $p_{i_r} = 0.99$ the last term will be an extra safety to account for uncertainty. The conditional mean state is calculated by (15a) and is linear in future inputs while the conditional state covariance is calculated by (15b) and is independent of inputs. The initial values $\hat{x}_{k|k}, P_{k|k}$ comes from the KF.

$$\hat{x}_{k+i+1|k} = A\hat{x}_{k+i|k} + Bu_{k+i} \quad (15a)$$

$$P_{k+i+1|k} = AP_{k+i+1|k}A^T + Q \quad (15b)$$

The literature on SMPC referenced in this paper raises a so called *open loop feasibility problem* which is the following. If the system dynamics is not well damped but maybe even unstable the conditional state covariance (15b) will increase quickly and in the unstable case the covariance becomes unbounded. This can very easily render the problem infeasible. The remedy for this suggested by many [8], [9], [10], [11], [12] is "Disturbance feedback control" which essentially uses state feedback to make the modes of the system more damped and hence reduce the growth of the covariance. However, obviously this is not a solution if the control is supposed to be based solely on constraints. Fortunately, as explained below, this covariance related feasibility problem is much less of a problem than stated in the literature.

It is important to observe the following differences between MPC and SMPC. Assume the model is perfect. If the MPC problem is infeasible at time k this will not change in the future provided it is completely deterministic with known initial state. If the SMPC problem is infeasible at time k this can change in the future for two reasons. At time

k consider the constraint (14d) defined by $(\hat{x}_{k+i|k}, P_{k+i|k})$, after j samples ($1 \leq j < i$) the constraint for the same state will be defined by $(\hat{x}_{k+i|k+j}, P_{k+i|k+j})$. Especially If j is close to i the state estimate can have changed but more importantly the covariance will be smaller. Consequently, a constraint that is infeasible at time k could very well end up feasible later at time $k + j$.

Based on the above insight this paper suggest the constraint (14d) to be modified to (16).

$$F_r \hat{x}_{k+i|k} \leq f_{i_r} - \phi^{-1}(p_{i_r}) \sqrt{F_r P_{k+\max(i, H_c)|k} F_r^T}, \quad (16a)$$

$$1 \leq H_c \leq H_p \quad (16b)$$

Notice that the update of the state covariance is truncated at prediction horizon H_c not primary to hinder the fast growth but because the covariance closer to the end of the prediction horizon H_p is not relevant as explained above. This introduces one more tuning parameter H_c on top of many others. This is still far simpler compared to the “disturbance feedback” suggested in the literature.

The literature presents the feasibility problem as unavoidable in SMPC. This is because the conditional probability of respecting limits p_{i_r} is assumed to be larger than $\frac{1}{2}$ such that $\phi^{-1}(p_{i_r})$ in (14d) is positive and the uncertainty part narrows the constraint. As demonstrated in the wind turbine example p_{i_r} can be smaller than $\frac{1}{2}$ which makes the feasibility problem disappear as this will then loosen the constraint.

D. Unconditional constraints probability approximation

To match an unconditional probabilistic constraint like (7) accurately some tuning of the conditional constraint probability is needed. As simulations or real experiment are often very time consuming it is necessary to have a simple way to get a good starting point. For this the following approximate method is developed.

Assume that the problem is feasible so the SMPC algorithm makes sure that the constraints (16) holds. Also assume there is a couple of interval constraints i.e. $F_r = -F_l$. Then the SMPC algorithm forces the conditional mean value $F_r \hat{x}_{k+i|k}$ to stay within the limits l_l, l_r (17).

$$l_l \leq F_r \hat{x}_{k+i|k} \leq l_r, \quad (17a)$$

$$l_l = f_{i_l} - \phi^{-1}(p_{i_l}) \sqrt{F_l P_{k+\max(i, H_c)|k} F_l^T}, \quad (17b)$$

$$l_r = f_{i_r} - \phi^{-1}(p_{i_r}) \sqrt{F_r P_{k+\max(i, H_c)|k} F_r^T}, \quad (17c)$$

Approximate the unconditional distribution of $\mu = F_r \hat{x}_{k+i|k}$ with a distribution $p(\mu)$ with support $[l_l, l_r]$ then the unconditional probability can be approximated as (18).

$$\begin{aligned} P(F_r x_{k+i} \leq f_r) &= \int_{l_l}^{l_r} P(F_r x_{k+i} \leq f_r | \mu) p(\mu) d\mu \\ &= \int_{l_l}^{l_r} \phi \left(\frac{f_r - \mu}{\sqrt{F_r P_{k+i|k} F_r^T}} \right) p(\mu) d\mu \end{aligned} \quad (18)$$

The method works by starting with a conditional probability $p_{i_l} = p_{i_r} = p$ in (17) and calculate the unconditional probability in (18), then adjust p in (17) and continue until a satisfactory result is reached. Notice the relation between the probabilities is monotone. See the wind turbine example for more details.

In practice the distribution of μ is unknown but a uniform or truncated Gaussian distribution with support $[l_l, l_r]$ will work. There is also the choice of constraint r and time horizon i to choose. If the chosen constraint is open in one end the distribution of μ for that part has to be chosen according to the application in question.

III. SIMPLIFIED WIND TURBINE EXAMPLE

As explained in the introductions WT control in high wind is mainly designed to keep the rotational speed within limits with a high probability. Consequently, SMPC control could be a beneficial method for this.

This simplified WT model is useful for demonstrating some of the methods presented above and for showing the qualitative effects of including or excluding probabilistic constraints. However, the model is too simple for a quantitative assessment of WT control which is the reason why proper statistical treatment of simulation results is avoided.

A. Linearized wind turbine model

To focus on speed control only the WT is modeled as one lumped inertia cast to the rotor speed side (19) [16, Sect. 7.3] and the wind speed is modeled with a first order stochastic differential equation (SDE) model for turbulence (20a) and a Wiener process (20b) for the low frequent wind speed part [17]. This Wiener process, or integrated white noise, also gives the MPC “integral action” similar to the method found in [1, sect. 7.4]. To align with the analysis for linear systems the non linear aerodynamic effects is linearized (19e)- (19j). Table I explain the notation. The WT is the NREL 5MW virtual turbine [16].

$$I \dot{\omega} = T_r - T_g, \quad (19a)$$

$$T_r = \frac{1}{2} \rho v^3 A C_p(\lambda, \beta) \frac{1}{\omega}, \quad (19b)$$

$$T_g = \frac{P_n}{\omega}, \quad (19c)$$

$$\lambda = \frac{\omega R_r}{v}, \quad (19d)$$

$$\delta \dot{\omega} \simeq c_\omega \delta \omega + c_\beta \delta \beta + c_v \delta v, \quad (19e)$$

$$\delta x = x - x_o \quad x_o = \text{operation value}, \quad (19f)$$

$$c_x = \frac{1}{I} \frac{\partial(T_r - T_g)}{\partial x} \quad (19g)$$

$$c_\omega = \frac{\rho A}{2I} v^3 \left(-C_p(\lambda, \beta) \frac{1}{\omega^2} + \frac{\partial C_p}{\partial \lambda} \frac{R_r}{v} \frac{1}{\omega} \right) + \frac{P_n}{I \omega^2}, \quad (19h)$$

$$c_\beta = \frac{\rho A}{2I} v^3 \frac{1}{\omega} \frac{\partial C_p}{\partial \beta}, \quad (19i)$$

$$c_v = \frac{\rho A}{2I} \frac{1}{\omega} \left(3v^2 C_p(\lambda, \beta) - \frac{\partial C_p}{\partial \lambda} w R_r v \right) \quad (19j)$$

$$dv_t = -a(v_m)v_t dt + dw_t, \quad (20a)$$

$$dv_m = dw_m, \quad (20b)$$

$$v = v_t + v_m \quad (20c)$$

$$A = e^{A_c T_s}, \quad B = \int_0^{T_s} e^{A_c \tau} B d\tau, \quad (22a)$$

$$Q = \int_0^{T_s} e^{A_c \tau} Q_c (e^{A_c \tau})^T d\tau, \quad (22b)$$

$$C = \begin{pmatrix} 1 & 0 & 0 \end{pmatrix} \quad (22c)$$

Symbol	Description	Unit	Value
Variables			
ω	Rotor speed	rad/s	1.267
T_r	Aerodynamic rotor torque	Nm	3.946e+06
T_g	Generator torque (rotor side)	Nm	3.946e+06
v	Wind speed	m/s	15
v_m	Wind speed - slow part	m/s	15
v_t	Wind speed - turbulence	m/s	0
C_p	Efficiency		0.2049
λ	Tip speed ratio		5.322
β	Blade pitch	deg	10.45
w_m	Wiener process - slow part	m/s	
w_t	Wiener process - turbulence	m/s	
Parameters			
P_n	Nominal power	w	5e+06
I	Lumped inertia	kgm ²	4.047e+07
ρ	Air density	kg/m ³	1.223
A	Rotor area	m ²	12469
R_r	Rotor radius	m	63
c_ω	ω gain	1/s	-0.07077
c_β	β gain	rad/(s ² grad)	-0.01571
c_v	v gain	rad/(sm)	0.02619
q_m	Incremental cov. - slow part	(m/s) ²	0.006667
L	Turbulence length par.	m	340.2
t_i	Turbulence intensity		0.1
q_t	Incremental cov. - turbulence	(m/s) ²	0.3117
$a(v_m)$	Turbulence model bandwidth	rad/s	0.06926
T_s	Sample time	s	0.1
R	Measurement noise var.	(rad/s) ²	0.0001606

TABLE I

WIND TURBINE MODEL VARIABLES AND PARAMETERS. THE TURBINE IS THE NREL 5MW VIRTUAL TURBINE [16]. THE VARIABLE VALUES ARE THE OPERATIONAL POINT VALUES. SAMPLE TIME AND MEASUREMENT NOISE VARIANCE ARE ALSO INCLUDED.

Combining the linear WT model (19e) and the wind model (20) the 3 order linear SDE (21) is obtained which can be sampled with sampling step T_s to obtain the standard discrete time SS model (1) where the parameters are given by (22) [18]. The measurement model consist of measuring the rotor speed plus noise (22c). The wind speed could be included as a measurement with large uncertainty. This is avoided here as the simple standard WT controller only uses rotational speed.

$$dx = (A_c x + B_c u)dt + dw, \quad (21a)$$

$$x = (\omega \quad v_t \quad v_m)^T, \quad u = \beta, \quad (21b)$$

$$A_c = \begin{pmatrix} c_\omega & c_v & c_v \\ 0 & -a(v_m) & 0 \\ 0 & 0 & 0 \end{pmatrix}, \quad (21c)$$

$$B_c = (c_\beta \quad 0 \quad 0)^T, \quad (21d)$$

$$w \sim W(Q_c), \quad Q_c = \text{diag}(0, q_t, q_m) \quad (21e)$$

For WT control it does not make sense to penalize pitch but only pitch changes. To transform the model (1) into one with input changes as input an integrator is appended to the dynamics and the previous input is appended to the state [1, sect. 2.4] to give the system (23).

$$x'_k = (x_k \quad u_{k-1})^T, \quad u'_k = u_k - u_{k-1}, \quad (23a)$$

$$A' = \begin{pmatrix} A & B \\ \underline{0} & I \end{pmatrix}, \quad B' = \begin{pmatrix} B \\ I \end{pmatrix}, \quad (23b)$$

$$C' = (C \quad \underline{0}), \quad Q' = \begin{pmatrix} Q & \underline{0} \\ \underline{0} & \underline{0} \end{pmatrix} \quad (23c)$$

B. Control problem

The chosen control problem specifications are: maintain the rotor speed within $\pm 10\%$ of the nominal value with a probability of 0.9, within the interval there are no cost on rotor speed, there are no cost on pitch but there are quadratic cost on pitch speed which also is assumed to have a limit of 8 deg/sec [16] in both directions. The constraint probability of 0.9 is chosen low to avoid too large uncertainty when estimating this based on simulations in section III-D.

C. Feasibility problem

Figure 1 shows the multi step state predictions std. calculated using (15b). The wind predictions start from a relatively high value as there are no direct wind measurement. The turbulence std. increases toward the stationary value at turbulence intensity times mean wind speed i.e. 1.5 m/s. The slow wind part std. keeps increasing as it is a Wiener process. The rotor speed std. start from nearly zero due to the low measurement noise and grow from there.

In this case the rotor speed is limited to a range of 10% from the nominal value which means that (14d) becomes (24) so when the right hand side becomes negative the problem is infeasible also without input constraints. With $p = 0.95$ this happens, according to (15b), after step 44 i.e. 4.4 sec. which means that H_c in (16) should not exceed 44. For this example with max input at 8 deg/sec 44 steps is actually feasible. Reducing the input max to 0.8 deg/sec 44 steps is infeasible but 30 steps is feasible.

$$|\hat{x}_{k+i|k}| \leq f - \phi^{-1}(p) \sqrt{P_{k+i|k,1}} \quad (24)$$

The above is an example of an approach which in many cases can determine the limit where covariance updating leads to infeasibility.

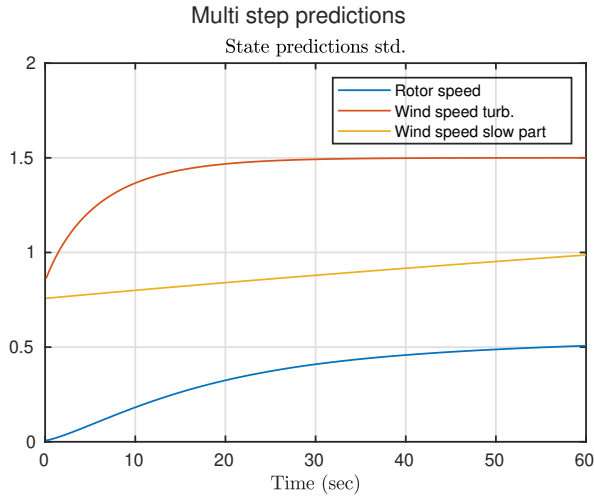


Fig. 1. Multi step state predictions std. The starting state covariance is from the KF after running a SMPC controller for 600 sec.

D. SMPC control solutions

In this section two SMPC controllers are compared. The first one have no rotor speed penalty but only constraints (C-SMPC). The second is the opposite with no rotor speed constraint but only penalty (P-SMPC).

For both controllers the prediction horizon H_p is chosen to 5 sec. or 50 samples as this is similar to one rotor revolution. The covariance update in (16) is truncated after 1 sec i.e. $H_c = 10$. Also the input penalty T_i in (2a) is fixed at 1.

Starting with the C-SMPC the conditional probability given the unconditional constraint probability 0.95 must be found. The initial value is found using the method described in section II-D. Fortunately there is effectively only one state constraint. It seems reasonable to assume the relevant horizon is within the first sec. or so. Figure 2 shows the tuning process. Initially conditional probability at 0.95 was inserted in (17)-(18) which gave the upper blue line with far to high unconditional probability as expected (12b). The conditional probability was then reduced until (17)-(18) gave unconditional probability close to 0.95 for close to 10 samples. This was obtained with conditional probability at 0.25 (red line) which was then simulated with the result of a unconditional probability at 0.977 which is still higher than the target at 0.95. The simulated unconditional probability at 0.977 (green line) matches the approximation (red line) between sample 1 and 2. Assuming this holds in general, conditional probability is reduced until the target 0.95 is obtained between sample 1 and 2 which happens for conditional probability at 0.03 (yellow line). Simulation results for conditional probability at 0.03 gave unconditional probability at 0.949 which is sufficiently close to the target 0.95. Notice that it took only two simulations to find the conditional probability 0.03 given the target unconditional probability and that this conditional probability was far from the target unconditional probability.

The tuning of the P-SMPC controller was more time consuming as the penalty on the rotor speed had to be

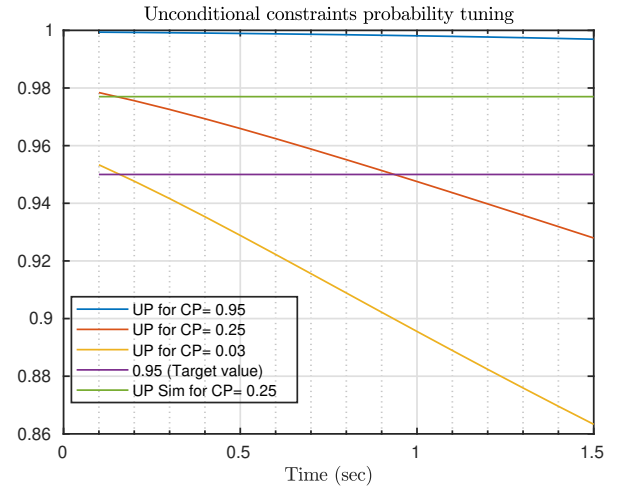


Fig. 2. Unconditional constraints probability tuning. Se text for details. Notice this is single (one sided) constraints.

increased from 0 until the single constraint probability had reached 0.95 and this all has to be done using simulation. A sufficiently close result is obtained by $S_{i11} = 0.31$ in (2a) which gives unconditional probability at 0.949. The simulated single side unconditional probability is obtained as the average of the upper and lower limit probabilities.

The result of simulating the controllers are show in the time plots in figure 3 where a common simulated wind is used. The pitch increments most clearly shows the difference between the controllers. The C-SMPC clearly have periods (e.g. 400-500 sec.) where it is zero or very small and then high values at the ends of these intervals. This corresponds to the pitch being close to constant in these intervals and then changing fast in the ends of the intervals. The pitch for the two controllers are similar for the low frequency part as the pitch has to correspond to the wind speed. The rotor speed time plots appears quit similar for the controllers.

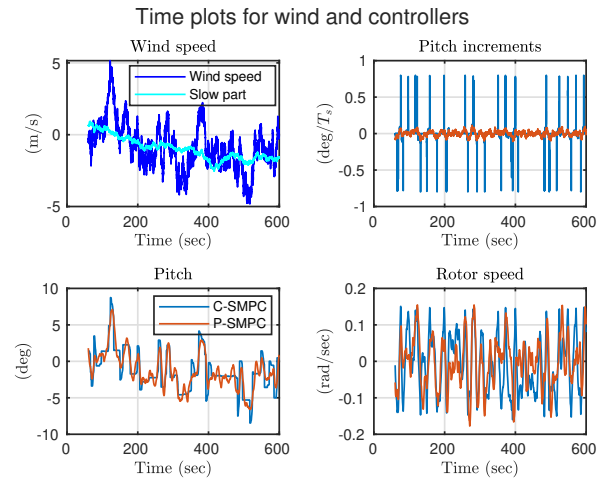


Fig. 3. Time plots for wind speed, pitch increments, pitch and rotor speed. The legend for pitch is common for the last three sub-plots. The first 10% of the samples are discarded to avoid initial effects. The simulated wind speed is common for both controllers.

The histograms for the same data are seen in figure 4. The pitch increments are seen to have much longer tails compared to a Gaussian distribution for the C-SMPC whereas it seems Gaussian for the P-SMPC. Notice that the tails are bounded by the pitch speed so the pitch increments can be made less jumpy by limiting the pitch speed to less than the maximum 8 deg/sec. For the pitch the non Gaussianity has almost disappeared. Perhaps the distributions are a little skew do to the drifting slow part of the wind. From the rotor speed histogram it is clear that the C-SMPC gives less tails compared to the P-SMPC which seems Gaussian.

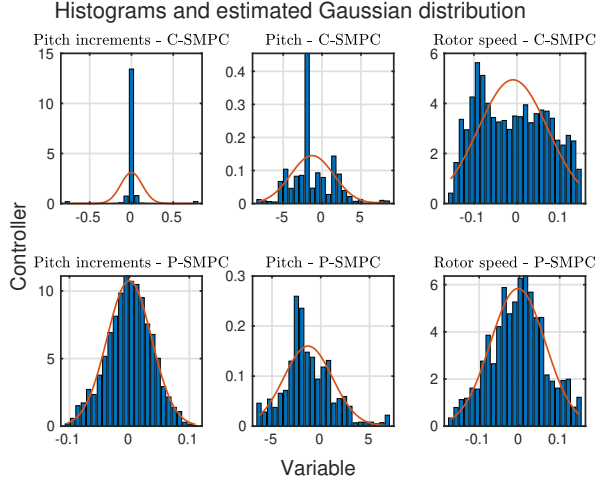


Fig. 4. Histograms for pitch increments, pitch and rotor speed shown in figure 3. The red line is the estimated Gaussian distribution.

Statistics for the signals in the figures are shown in table II. The statistics supports the observations already made. For example the kurtosis for pitch increments is around 3, as for a Gaussian distribution, for P-SMPC where as it is far higher for C-SMPC which also leads to a far higher RMS for C-SMPC compared to P-SMPC. For the controlled variable, rotor speed, P-SMPC shows around 10% lower RMS even though the fraction of respected constraints are close to 0.9 for both controllers. This is not a surprise as the P-SMPC newer gets near the input constraints and the horizon is quit long so it is similar to a LQG controller which is optimal in RMS (MSE) sense.

However, as stated in section I the purpose for WT control is to keep the rotor speed within limits and minimize the fatigue loads. A good assessment of relevant fatigue needs a model of higher fidelity. For the current simple model there are at most two load proxies that can be obtained. For the load on the pitch system the total traveled pitch is relevant. This is include in table II as ASum (Absolute sum of pitch increments). Also the pitch can be considered a proxy for blade loading. This motivates the scaled damage equivalent load (DEL) included in the table. This measure is based on rain flow counting using MATLAB RAINFLOW and the below formula where n_i is the count of range f_i and m is

the Wöhler coefficients which here is 10 as for glass fiber.

$$\text{DEL} = \left(\sum_i n_i f_i^m \right)^{\frac{1}{m}}. \quad (25)$$

As seen, these two load proxies are quit similar for the controllers even though the tendency is in favor of the P-SMPC.

Var	Ave	RMS	MAD	Kur	UP	ASum	DEL
C-SMPC							
ω	-0.009	0.081	0.070	1.850	0.898		
$\Delta\beta$	0.000	0.129	0.030	34.751	0.000	162.400	
β	-1.270	2.751	2.138	3.926			16.552
P-SMPC							
ω	-0.004	0.073	0.058	2.681	0.898		
$\Delta\beta$	0.000	0.036	0.029	2.803	0.000	154.450	
β	-1.299	2.493	1.909	3.938			13.493

TABLE II

PERFORMANCE OF CONTROLLERS. LEGENDS: AVE: AVERAGE, RMS: RMS, MAD: AVERAGE ABSOLUTE DISTANCE, KUR: KURTOSIS, UP: UNCONDITIONAL FRACTION (PROBABILITY) OF RESPECTING CONSTRAINT, ASUM: ACCUMULATED SUM I.E. TRAVELED PITCH, DEL: DAMAGE EQUIVALENT LOAD BASED ON RAINFLOW COUNTING FOR PITCH (25).

In summary, the unconditional probability for respecting rotor speed constraint can be obtained by varying the amount of penalty and probabilistic constraint on rotor speed and limits on pitch speed. Even though controllers give the same unconditional probability the distributions of pitch increments, pitch and rotor speed can be very different. Whether including probabilistic constraints can lead to reduced fatigue for WT can only be investigated using a model of higher fidelity which will be a topic for future research.

IV. CONCLUSION

This paper contributes to three challenges using probabilistic constraints in SMPC and illustrates the points made with an example from WT control.

The current research on SMPC identifies the growth of the prediction covariance as a major problem as it is claimed to generally lead to infeasibility for relevant predicting horizons. This paper explains that the *conditional probability* of respecting the constraints can be smaller than 0.5 even if the *unconditional probability* is close to 1. In this case the constraints are loosened not tightened when the prediction variance increase and there is no feasibility problem at all. In case the conditional probability of respecting the constraints are larger than 0.5 so the constraints are tightened the solution is to truncated the covariance update after a suitable number of samples as the controller after some samples anyway has a better prediction.

The *unconditional probability* of respecting constraints are relevant in applications but the design parameter is the probability *conditioned on present measurements*. This is generally a overseen problem. The paper develops an approximate relation between the two probabilities which

makes it easy to find a good initial value for the conditional probability to test and tune in practice or simulation as demonstrated in the application example.

An important point made in the paper is that a given *unconditional probability* for respecting constraints can be obtained by many controller designs. For conventional set point following controllers the distribution of all signals will be close to Gaussian if the disturbance are and the system is close to linear. The SMPC controller that mainly, or only, use constraints to limit the variation of the controlled variable will have clearly non Gaussian distributions for both inputs and controlled variables. This is demonstrated in the WT application example. The difference between constraint based SMPC and conventional controllers are in the distributions and in the ease of design. This paper have given contributions to the latter as demonstrated in the simple WT example.

However, if the change in distributions can be exploited for improving fatigue and WT performance in general calls for a more sophisticated model which is a subject for future research.

REFERENCES

- [1] J. M. Maciejowski, *Predictive Control with Constraints*. Prentice Hall, 2002.
- [2] "ICONIC smart, aware, integrated wind farm control interacting with digital twins," Project 101122329 Funded by the European Union, 2023.
- [3] T. Burton, N. Jenkins, D. Sharpe, and E. Bossanyi, *Wind Energy Handbook*, 2nd ed. John Wiley, 2011.
- [4] G. A. M. van Kuik, J. Peinke, R. Nijssen, D. Lekou, J. Mann, J. N. Sørensen, C. Ferreira, J. W. van Wingerden, D. Schlipf, P. Gebrad, H. Polinder, A. Abrahamsen, G. J. W. van Bussel, J. D. Sørensen, P. Tavner, C. L. Bottasso, M. Muskulus, D. Matha, H. J. Lindeboom, S. Degraer, O. Kramer, S. Lehnhoff, M. Sonnenschein, P. E. Sørensen, R. W. Küneke, P. E. Morthorst, and K. Skytte, "Long-term research challenges in wind energy - a research agenda by the european academy of wind energy," *WIND ENERGY SCIENCE*, vol. 1, pp. 1–39, 2016.
- [5] F. Zahle, A. Barlas, K. Lønbæk, P. Bortolotti, D. Zalkind, L. Wang, C. Labuschagne, L. Sethuraman, and G. Barter, *Definition of the IEA Wind 22-Megawatt Offshore Reference Wind Turbine*. Technical University of Denmark, 2024, dTU Wind Energy Report E-0243 IEA Wind TCP Task 55.
- [6] W. Engels, S. Subhani, H. Zafar, and F. Savenije, "Extending wind turbine operational conditions; a comparison of set point adaptation and lqg individual pitch control for highly turbulent wind," in *Journal of Physics: Conference Series*, vol. 524. The Science of Making Torque from Wind 2014 (TORQUE 2014) IOP Publishing, 2014.
- [7] P. F. Odgaard, T. Knudsen, A. Overgaard, H. Steffensen, and H. Jørgensen, "Importance of dynamic inflow model predictive control of wind turbines," in *9th IFAC Symposium on Control of Power and Energy Systems CPES 2015, New Delhi, India, December 9-11 2015*, ser. IFAC Workshop Series, vol. 48, no. 30, IFAC. IFAC, 2015, pp. 90–95.
- [8] M. Farina, L. Giulioni, and R. Scattolini, "Stochastic linear model predictive control with chance constraints - a review," *Journal of Process Control*, vol. 44, pp. 53–67, 2016. [Online]. Available: <https://www.sciencedirect.com/science/article/pii/S0959152416300130>
- [9] R. D. B. Joel A. Paulson, Edward A. Buehler and A. Mesbah, "Stochastic model predictive control with joint chance constraints," *International Journal of Control*, vol. 93, no. 1, pp. 126–139, 2020. [Online]. Available: <https://doi.org/10.1080/00207179.2017.1323351>
- [10] P. J. Goulart, E. C. Kerrigan, and J. M. Maciejowski, "Optimization over state feedback policies for robust control with constraints," *Automatica*, vol. 42, no. 4, pp. 523–533, 2006. [Online]. Available: <https://www.sciencedirect.com/science/article/pii/S0005109806000021>
- [11] T. A. N. Heirung, J. A. Paulson, J. O'Leary, and A. Mesbah, "Stochastic model predictive control - how does it work?" *Computers & Chemical Engineering*, vol. 114, pp. 158–170, 2018, fOCAPO/CPC 2017. [Online]. Available: <https://www.sciencedirect.com/science/article/pii/S0098135417303812>
- [12] E. González, J. Sanchis, S. García-a Nieto, and J. Salcedo, "A comparative study of stochastic model predictive controllers," *Electronics*, vol. 9, no. 12, 2020. [Online]. Available: <https://www.mdpi.com/2079-9292/9/12/2078>
- [13] A. Nemirovski and A. Shapiro, "Convex approximations of chance constrained programs," *SIAM Journal on Optimization*, vol. 17, no. 4, pp. 969–996, 2006.
- [14] T. Knudsen and J. Leth, "Stochastic mpc using the unscented transform," in *2018 Annual American Control Conference, ACC 2018*, IEEE. IEEE, 2018, pp. 4718–4724.
- [15] A. Ben-Tal, L. E. Ghaoui, and A. Nemirovski, *Robust Optimization*, ser. Princeton Series in Applied Mathematics. Princeton University Press, 2009, vol. 28.
- [16] J. Jonkman, S. Butterfield, W. Musial, and G. Scott, "Definition of a 5-mw reference wind turbine for offshore system development," National Renewable Energy Laboratory, 1617 Cole Boulevard, Golden, Colorado, USA, Tech. Rep. NREL/TP-500-38060, 2009.
- [17] T. Knudsen, M. Soltani, and T. Bak, "Prediction models for wind speed at turbine locations in a wind farm," *Wind Energy*, vol. 14, pp. 877–894, 2011, published online in Wiley Online Library (wileyonlinelibrary.com). DOI: 10.1002/we.491.
- [18] K. J. Åström, *Introduction to Stochastic Control Theory*, ser. Mathematics in science and engineering, R. Bellman, Ed. Academic Press, 1970, vol. 70.